PCCP

Accepted Manuscript




ROYAL SOCIETY OF CHEMISTRY

www.rsc.org/pccp

# PCCP Guidelines for Referees

***Physical Chemistry Chemical Physics*** **(*PCCP*) is a high quality journal with a large international readership from many communities**

Only very important, insightful and high-quality work should be recommended for publication in *PCCP*.

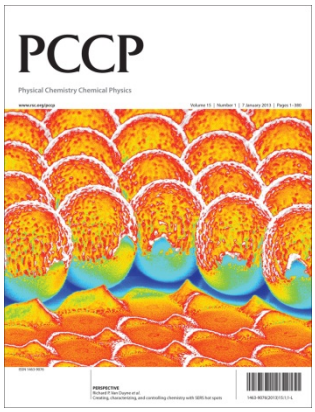


**To be accepted in *PCCP*** - a manuscript must report:

- Very high quality, reproducible new work
- **Important new physical insights** of significant general interest
- A novel, stand-alone contribution

**Routine or incremental work** should not be recommended for publication. Purely synthetic work is not suitable for PCCP

If you rate the article as 'routine' yet recommend acceptance, please give specific reasons in your report.

**Less than 50%** of articles sent for peer review are recommended for publication in *PCCP*. The current PCCP Impact Factor is 3.83

*PCCP* is proud to be a leading journal. We thank you very much for your help in evaluating this manuscript. Your advice as a referee is greatly appreciated.

With our best wishes,

Philip Earis (pccp@rsc.org)
Managing Editor, PCCP

Prof Daniella Goldfarb
Chair, PCCP Editorial Board

**General Guidance (For further details, see the RSC's Refereeing Procedure and Policy)**

Referees have the responsibility to treat the manuscript as confidential. Please be aware of our **Ethical Guidelines** which contain full information on the responsibilities of referees and authors.

*When preparing your report, please:*
• Comment on the originality, importance, impact and scientific reliability of the work;
• State clearly whether you would like to see the paper accepted or rejected and give detailed comments (with references) that will both help the Editor to make a decision on the paper and the authors to improve it;

*Please inform the Editor if:*
• There is a conflict of interest;
• There is a significant part of the work which you cannot referee with confidence;
• If the work, or a significant part of the work, has previously been published, including online publication, or if the work represents part of an unduly fragmented investigation.

*When submitting your report, please:*
• Provide your report rapidly and within the specified deadline, or inform the Editor immediately if you cannot do so. We welcome suggestions of alternative referees.

Journal Name

RSCPublishing

ARTICLE

# Complexes Formed between DNA and Poly(amido amine) Dendrimers of Different Generations – modelling DNA wrapping and penetration

Cite this: DOI: 10.1039/xoxxooooox

Received ooth January 2012,
Accepted ooth January 2012

DOI: 10.1039/xoxxooooox

www.rsc.org/

Khawla Qamhieh,[a,b] Tommy Nylander,*[a] Camilla F. Black,[c] George S. Attard,[c] Rita S. Dias,[a,d] and Marie-Louise Ainalem [a,e],

This study deals with the build up of biomaterials consisting of biopolymers, namely DNA, and soft particles, poly(amido amine) (PAMAM) dendrimers, and how to model their interactions. We adopted and applied an analytical model to provide further insight on the complexation between DNA (4331 bp) and positively charged PAMAM dendrimers of generations 1, 2, 4, 6 and 8, previously studied experimentally. The theoretical models applied describe the DNA as a semiflexible polyelectrolyte that interacts with dendrimers considered as either hard (impenetrable) spheres or as penetrable and soft spheres. We found that the number of DNA turns around one dendrimer, thus forming a complex, increases with dendrimer size or generation. The DNA penetration required for the complex to become charge neutral depends on the dendrimer generation, where lower generation dendrimers requires little penetration to give charge neutral complexes. High generation dendrimers display charge inversion for all considered dendrimer sizes and degrees of penetration. Consistent with the morphologies observed experimentally for dendrimer/DNA aggregates, where highly ordered rods and toroids are found for low generation dendrimers, the DNA wraps less than one turn around the dendrimer. Disordered globular structures appear for high generation dendrimers, where DNA wraps several turns around the dendrimer. Particularly noteworthy is that the dendrimer generation 4 complexes, where the DNA wraps about one turn around the dendrimers, are borderline cases and can form all types of morphologies.The net-charges of the aggregate have been estimated by zeta potential measurements and are discussed within the theoretical framework.

## Introduction

The development of novel biomaterials for medical applications with controlled nanostructure and organisation, a branch on material science often referred to as nanomedicine, is opening up new avenues for disease prevention, diagnosis and treatment. It is becoming increasingly feasible to use structures engineered at the molecular level to monitor, repair and construct at the cellular level.[1-3] One of the ultimate goals is the detection of a disease in its earliest stage which allows for rapid and targeted treatment.[4] This entails the delivery of a therapeutic agent to the site of its action, which often poses major challenges that can preclude the use of a drug in the clinic. The issue of efficient and safe delivery is particularly important in the field of gene therapy, and several nanotechnology approaches to packaging nucleic acids have been reported. Dendrimers have emerged as effective materials for delivering DNA for gene therapy. Dendrimers are branched polymeric molecules which have a specific size and shape, and which can be synthesized with a very narrow weight distribution. Thanks to their unique molecular structure, dendrimers are probably the most promising examples of synthetic molecules with proven great potential as delivery vectors for gene transfection.[3,5-11] Transfection efficiency and functionality of dendrimer/DNA aggregates have been found to depend on the structure, size, and the charge density of the dendrimers.[12-17]

The aim of this study is to provide further insights into the formation and structure of complexes and aggregates composed of DNA and PAMAM dendrimers of different generations by applying a relatively simple and applicable analytical model. Here we use the term complex to refer to the entity formed by one dendrimer and the part of a DNA molecule that wraps around it. The structure formed between the entire DNA molecule and multiple dendrimers is termed an aggregate. Our focus is on DNA and dendrimers but our approach could easily be extended to any interacting system consisting of charged biopolymers and oppositely charged particles.

Upon condensation of a double stranded DNA molecule (e.g. by oppositely charged molecules) the dramatic decrease in the volume occupied by the DNA results in a loss of configurational entropy.[18] In addition the double helix is bent and intramolecular electrostatic repulsions are expected to

increase due to the more compact structure. To overcome these energy barriers, which oppose DNA compaction, oppositely charged compacting agents (e.g. dendrimers) might be used. The Manning counterion condensation theory states that about 90% of the DNA charges need to be neutralized for the DNA to condense.[19] This correlation theory, which has been studied intensively by computer simulations,[20-26] is usually applied to describe the overcharging of an impenetrable macroion and accounts for the interaction between a small excess of the opposite charge on the macro-ion surface.[27-29] Both theory[28,29] and Monte Carlo simulations[23,26] show that charged hard spheres can become overcharged by oppositely charged linear polyelectrolytes (LPE) with constant charge density. The overcharging phenomenon in complexes formed between dendrimers and an LPE has been predicted by brownian dynamics simulations,[30] as well as by using an analytical model applied to poly(amido amine) (PAMAM) dendrimers complexed with DNA.[31]

PAMAM dendrimers have an ethylenediamine core and primary amine functional groups at each branch end-point and tertiary amine groups at each branch dividing point. This architecture creates internal cavities with a different microenvironment within the dendrimer core, compared to the shell, as a consequence of the lower density at the center of the molecule.[32] The conformation of dendrimers depends on their generation, i.e. dendrimers of higher generations may be considered sphere-like whereas smaller dendrimers adopt a flatter shape,[33-35] and are also less rigid.[36,37] Unlike a hard sphere a dendrimer is flexible and does not possess a clearly defined surface, i.e. the surface structure allows for penetration of a LPE. As a result modelling and prediction of the adsorption of a LPE onto a dendrimer is challenging.

**Table 1.** Properties of the PAMAM dendrimers of different generation, *G*, investigated in this study [a]

| Dendrimer | $R_o$ (*nm*) | $Z$ (*e*) | $\sigma$ ($e/nm^2$) | $l_{iso}$ (*nm*) |
|---|---|---|---|---|
| G1 | 1.10 | 8 | 0.52 | 1.37 |
| G2 | 1.45 | 16 | 0.60 | 2.72 |
| G4 | 2.25 | 64 | 1.00 | 10.88 |
| G6 | 3.35 | 256 | 1.81 | 43.52 |
| G8 | 4.85 | 1024 | 3.46 | 174.08 |

[a] The radius of the dendrimer is defined as $R_o$ and the number of charged groups on the dendrimer is *Z*. $\sigma$ is the surface charge density of the dendrimer. $l_{iso}$ is the isoelectric length of the DNA, i.e. the length of the double stranded DNA required to neutralize the charge of the different dendrimer generations.

The condensation of DNA using PAMAM dendrimers has been intensively studied experimentally and shown to be a cooperative process, i.e. giving rise to coexistence of free DNA, which adopts a random coil conformation, and fully condensed DNA molecules at intermediate charge ratios.[38,39] The charge ratio ($r_{charge}$) is defined as the ratio between the charged groups on the dendrimer surface and the phosphate groups on the DNA backbone, i.e. ($r_{charge}$) = $n(NH_3^+)/n(PO_4^-)$. The number of dendrimers bound per DNA molecule has been shown to decrease for higher dendrimer generations, remaining, however, independent of the charge ratio in dilute solutions at low charge ratios ($r_{charge} < 1$).[38,39] The morphologies of the aggregates formed between DNA and PAMAM dendrimers at these low charge ratios have furthermore been shown to depend on the dendrimer generation. Low dendrimer generation/DNA aggregates give rise to rods and toroids, while high generations cause the formation of globular and disorded structures.[39] PAMAM dendrimers also protect DNA against DNase activity and reduce in vitro gene transcription.[40-42]

In order to understand the DNA condensation process using dendrimers, it is important to better understand why these different morphologies are formed and to reveal how these structures are affected by dendrimer size, charge, and surface charge density at low $r_{charge}$ (<1). It is also important to determine the number of dendrimers that bind to each DNA molecule and to estimate the net charge of aggregates composed of one DNA chain and multiple dendrimer molecules. A theoretical model of the complex formation was developed by Schiessel et al..[43] We previously used this model to explore the effect of the DNA length on compaction using G4 dendrimers,[31] and we will therefore adopt and apply this model in the present study. The modelling will be based on experimental data obtained for the interaction between PAMAM dendrimers of generation 1 (G1), 2 (G2), 4 (G4), 6 (G6) or 8 (G8) and DNA, see Table 1. The model will be used to determine the charge of both the complexes and the aggregates. It will also be possible to elucidate to what degree the DNA molecule is wrapped around a dendrimer. The obtained results will be used to better understand how the experimentally observed morphologies depend on the dendrimer generation.[39,44,45] In addition to the theoretical model applied we will use previously obtained experimental data as well as recently recorded data on the charge of dendrimer/DNA aggregates using zeta potential measurements.

## Experimental

### Experimental background

The composition and morphology of aggregates formed between linearized DNA plasmids (4331 base pairs (bp)) and PAMAM dendrimers of generation 1, 2, 4, 6 and 8 have been thoroughly studied in aqueous solutions containing 10 mM sodium bromide, NaBr, at low $r_{charge}$ (<1).[39,44,45] Cryogenic transmission electron microscopy (cryo-TEM) and dynamic light scattering (DLS) were used to reveal that the lower dendrimer generations give rise to well-defined aggregates, that is G1 and G2 induce the formation of well-structured rods and toroids. For the higher generation dendrimers (G6, G8), globular and less well-defined aggregates are formed. The intermediate dendrimer generation, G4, appears to behave as a border case, where a range of morphologies (globules as well as toroids) are formed.

**Table 2.** The number of dendrimers bound per DNA molecule and the charge ratio of the dendrimer/DNA aggregate as estimated from experimental data at low $r_{charge}$ (<1) in dilute aqueous solutions.

| Dendrimer | G2 | G4 | G6 | G8 |
|---|---|---|---|---|
| $N_{exp}$ | 318 | 140 | 16 | 5 |
| $r_{charge}=N_{exp}Z_D/Z_{chain}$ | 0.58 | 1.03 | 0.47 | 0.59 |

[a] Data reproduced from Ainalem et al. [39,41] The experimentally determined number of dendrimers bound per DNA molecule is $N_{exp}$.[38] The charge ratio of the dendrimer/DNA aggregate is $r_{charge}$, $Z_D$ is the dendrimer charge number and $Z_{chain}$ (= 8662 for 4331 bp DNA) is the charge number of the DNA molecule.

The cooperative nature of the DNA condensation process, described above, was confirmed using cryo-TEM and DLS which displayed coexistence between dendrimer/DNA aggregates containing condensed DNA, and free extended DNA. Fluorescence spectroscopy was used to show that the number of dendrimers bound per DNA molecule decreased for larger dendrimers, but remained independent of $r_{charge}$. Previous experimental data are summarised in Table 2 and shows the number of dendrimers bound per condensed DNA molecule and the corresponding mean charge ratios of the aggregates.[39,41] These data indicate that all dendrimer generations give rise to aggregates with a negative net charge except for G4 dendrimers, which appear to form aggregates that are slightly positive.

### Materials

Luciferase T7 Control plasmid DNA (Promega), 4331 basepairs (bp), was amplified, linearized and purified as described in detail elsewhere.[39] PAMAM dendrimers of different generations (G1, G2, G4, G6, and G8) were purchased from Sigma and were received at high concentration (>5% w/w) in methanol. Before use, the methanol was removed under reduced pressure at room temperature after which the dendrimers were resolubilized in aqueous solutions (18.2 MΩ cm grade purity) containing 10 mM NaBr (Aldrich).
Dendrimer/DNA samples (2 mL) were prepared by adding dendrimer solutions of appropriate concentration into equal volumes of DNA solutions. The final DNA concentration was 0.025 mg $mL^{-1}$, which is well below the overlap concentration C* for the 4331 bp DNA molecule (estimated from the relative viscosity relationship of hard spheres).[39] The dendrimer concentration was varied in order to obtain samples with different charge ratios. The solutions were then left to equilibrate on a mixing board at 25 °C for at least 3 hours prior to analysis. All solutions contain 10 mM NaBr to prevent DNA denaturation. The pH of the samples was checked and found to be equal to 7 (±0.3) in all samples. The results were therefore interpreted assuming that all primary amine groups were protonated under the conditions used.

### Zeta potential measurements

Applying an electric field to a solution with charged particles induces the migration of the particles towards an oppositely charged electrode. The velocity (electrophoretic mobility) will depend on the strength of the field, the dielectric constant of the medium, the viscosity of the medium and the zeta potential. The zeta potential is the potential at the boundary called the slipping plane or hydrodynamic shear surrounding a particle surface. This boundary is located within the so-called diffuse layer where ions are less strongly attached compared to the inner region of strongly attached ions, often called the Stern layer. Ions within this boundary move with the particle and ions beyond this boundary do not. The zeta potential gives a semi-quantitative measure of the charge of the particles, in this case dendrimer/DNA aggregates, and an indication of the colloidal stability of the system, where approximately |30| mV usually means that the particles are sufficiently charged to repel one another, resulting in a stable system which will not coagulate. A positive zeta potential indicates a positive surface charge, and equally a negative zeta potential reflects a negative surface charge. Zeta potentials of around 0 mV, the isoelectric point, indicate that particles are close to neutral and, as such, the electrostatic repulsive interactions between the particles are weak and the systems are likely to coagulate.
The Henry equation (1) allows the zeta potential to be estimated from the electrophoretic mobility, $U_E$ ($m^2$ $s^{-1}$ $V^{-1}$), obtained experimentally:

$$U_E = \frac{2\varepsilon z f(\kappa a)}{3\eta} \qquad (1)$$

where ε is the dielectric constant of the solvent, z is the zeta potential (V), $\eta$ is the viscosity ($m^2$ $s^{-1}$) and $f(\kappa a)$ is Henry's function. Here $\kappa$ is the inverse Debye length ($\kappa^{-1}$) and $a$ is the radius of the particles. For $\kappa a \rightarrow \infty$, i.e. when the electrolyte concentration is moderate and the particles are large, $f(\kappa a) = 3/2$ (Smoluchowski approximation). For $\kappa a \rightarrow 0$, when the ionic strength is low and the particles are small, $f(\kappa a) = 1$ (Huckel approximation). A Zetasizer (Zetasizer Nano ZS from Malvern Instruments Ltd, Worshestershire, UK,) was used to measure the zeta potential of the dendrimer/DNA aggregates. Five repeat measurements were recorded for each sample and the obtained electrophoretic mobility of samples was converted into an average zeta potential value using the Helmholtz-Smoluchowski approximation assuming that the particles are spherical and large compared to the Debye length, $\kappa\kappa^{-1}$.

## Theoretical model

A theoretical model for the electrostatic complexation of spheres and chains under elastic stress, developed by Schiessel et al.,[43] was adopted. This model has previously been applied to describe G4/DNA aggregates for two DNA lengths, 2000 bp and 4331 bp.[31] Here it is applied to obtain a mechanistic understanding of how the dendrimer generation affects the formation and structure of the DNA-containing aggregates. PAMAM dendrimers of generations 1, 2, 4, 6 and 8 and DNA with 4331 bp were used in this study.

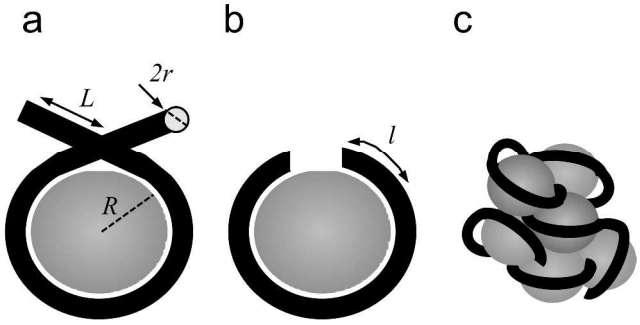


**Figure 1**. The proposed binding model between DNA, of contour length *L* and radius *r*, and PAMAM dendrimers modeled as hard spheres of radius *R*. In a) a segment of a DNA molecule is shown to wrap around one dendrimer. The DNA segments linking to the next dendrimer in an aggregate are shown. In b) a dendrimer/DNA complex consisting only of one dendrimer and the DNA segment of length, *l*, actually wrapping the dendrimer is visualized. In c) the dendrimer/DNA aggregate consisting of the entire DNA molecule and a multiple of dendrimers is shown. The model is in accordance with the cooperative binding model proposed by Örberg et al.[38]

The dendrimer was first considered as a hard sphere of radius *R* and charge *Ze* and the DNA as a linear polyelectrolyte of high

persistence length, which can be described as a semi-flexible rod of radius $r$ =1 nm and length $L>>R$. Figure 1 shows a schematic picture of the proposed binding model between dendrimers and DNA. We consider the 4331 bp DNA molecule used experimentally, having a contour length $L$ of 1472.5 nm. The charge of the DNA per unit length is $-e/b$ (=$-e$/0.17 nm) and the persistence length, $l_p$, is 50 nm, which is large compared to $R$. The fact that the experimental data were recorded in monovalent salt solutions is taken into account through the Bjerrum length, $l_B \equiv e^2/\epsilon k_B T$, and the Debye screening length, $\kappa^{-1}=(8\pi c_s l_B)^{-1/2}$, where $k_BT$ is the thermal energy and $c_s$ is the salt concentration. The experimental studies were performed in 10 mM NaBr aqueous solutions, which corresponds to $\kappa^{-1}$ = 3 nm, comparable to the size of the dendrimers but smaller than $L$. However, the derivation according to Schiessel et al. assumes that $\kappa^{-1}$ is large compared to the radius of the sphere (low ionic strength and small particles).[43] We argue that the assumption does not affect the results to a large extent as we regard the apparent radius of the dendrimer in the complex to be smaller than that of the free dendrimer. Furthermore the electrostatic term for the interaction within the aggregate is comparably small compared to other contributions. As DNA is a highly charged polyelectrolyte, the distance $b$ between charges is smaller than $l_B$= 0.7 nm using the dielectric constant of water at room temperature.[31,43]

**Calculation of the free energy for the dendrimer/DNA complex**

The model by Schiessel et al. for electrostatic complexation,[43] assumes that the total free energy of the system consisting of one dendrimer and one DNA segment can be expressed as a sum of four contributions, according to:

$$F(l) = F_{compl}(l) + F_{chain}(L-l) + F_{compl-chain}(l) + F_{elastic}(l) \quad (2)$$

where $l$ is the length of the DNA molecule wrapped around the sphere (dendrimer), and the remaining chain is of length ($L$-$l$). The complex, i.e., the sphere and corresponding wrapped chain has, thus, a total charge $eZ(l)=e(Z-l/b)$.
The first term, $F_{compl}(l)$, is the electrostatic charging free energy of a spherical complex of charge $eZ(l)$

$$F_{compl}(l) \cong \begin{cases} \frac{e^2 Z^2(l)}{2\varepsilon R}, |Z(l)| < Z_{max} \\ |Z(l)| k_B T \omega\big(Z(l)\big), |Z(l)| \gg Z_{max} \end{cases} \quad (3)$$

where, $\omega(Z(l))= 2\ln(|Z(l)|l_B\kappa^{-1}/R^2)$, is an entropic term that takes into account the confinement of the counterions condensed onto the sphere, in the case of a highly charged sphere, and $Z_{max}$ is the effective charge number of the sphere and is of the order of $\omega R/l_B$.[46]
The second term, $F_{chain}(L-l)$, is the total entropic electrostatic free energy of the remaining chain ($L$-$l$):

$$F_{chain}(L-l) \cong \frac{k_BT}{b}\Omega(r)(L-l) \quad (4)$$

where $\Omega(r)=2\ln(4\xi\kappa^{-1}/r)$ is a term describing the condensed DNA counterions, and $\xi \equiv l_B/b$ is the so-called Manning parameter.[19]
The third term, $F_{compl\text{-}chain}(l)$, is the electrostatic free energy of the interaction between the complex and the rest of the chain:

$$F_{compl-chain}(l) \cong Z^*(l) k_B T \ln(\kappa R) \quad (5)$$

where $Z^*(l)$ is the effective charge of the complex. For small complex charges, $|Z(l)|<Z_{max}$, which we will assume throughout, the effective charge obeys to $Z^*(l)= Z(l)$ .
The final term in Eq. 2, $F_{elastic}(l)$, is the elastic (bending) free energy and can be written according to:

$$F_{elastic}(l) \cong \frac{k_B T l_p}{R^2} l \quad (6)$$

Again, for $|Z(l)|<Z_{max}$, Eq. 2 can be written as:

$$\frac{F(l)}{k_BT} \cong \frac{l_B}{2R}\left(Z - \frac{l}{b}\right)^2 + \frac{Al}{b} + const \quad (7)$$

where all contributions which are linearly dependent on the wrapping length, $l$, i.e. the bending energy, electrostatic interaction between the complex and the un-complexed chain, and the release of the counterions of the chain, are combined in quantity $A$ given by:

$$A = \frac{l_p b}{R^2} - \ln(\kappa R) - \Omega \quad (8)$$

**Calculation of the free energy for the dendrimer/DNA aggregate**

For a system consisting of one DNA molecule and $N$ dendrimers, the total free energy can be expressed as:

$$F(N,l) = NF(l) + F_{int}(N,l) \quad (9)$$

where $F(l)$ is the total free energy of the dendrimer/DNA complex as expressed in Eq. 2 and $F_{int}$ is the interaction between the dendrimer spheres which are decorating the DNA molecule. $F_{int}$ is obtained as the sum of the electrostatic repulsion between all complexes within one DNA molecule. In the limit where the center-to-center distance between two neighboring (hard-sphere like) dendrimers with the same wrapping lengths, $D(N,l)=(L-Nl+2NR)$ is small compared to $\kappa^{-1}$ (very low ionic strength) but larger than $2R$ (no excluded volume effects), we can write the interaction force with the following approximation of an (repulsive) electrostatic interaction:

$$F_{int}(N,l) \cong \Lambda k_B T \frac{N l_B Z^2(l)}{D(N,l)} \quad (10)$$

where the quantity $\Lambda$ is a logarithmic factor of the order $\ln(\kappa^{-1}/D)$. Note that the expression for the interaction is an approximation. A more rigorous treatment of the electrostatic interaction force is not possible within our analytical framework. It is also worth noting that this term will be small if the complex charge is close to neutral, when the neighbouring spheres are sufficiently far apart, or at high ionic strength.
For $|Z(l)|<Z_{max}$, i.e. for large wrapping lengths, the total free energy of the dendrimer/DNA complex is quadratic in $l$ and Eq. 9 according to Eq. 7 can be expressed as:

$$\frac{F(N,l)}{k_BT} \cong \frac{l_{BN}}{2R} Z^2(l) + \frac{Al}{b} N - N\omega Z + \frac{\Lambda N^2 l_B Z^2(l)}{D(N,L)} + \ln(\kappa R)\, NZ \quad (11)$$

We will analyze the experimental results for the aggregates formed between dendrimers of different generations and DNA

by using the model by Schiessel et al.[43] with a minor change in Eq. 4. According to Manning, $(1-\xi^{-1})L/b$ counterions condense on a molecule and reduce its effective charge density to $l/l_B$.[19] Schiessel et al. ignored $\xi^{-1}$ in Eq. 4 because of the assumption that $\xi<<1$. For our system $\xi$= 4.12 and as a result, $\xi^{-1}$ is taken explicitly into account in the second term in Eq. 1, which states the total entropic electrostatic free energy of the remaining molecule ($L$-$l$). As a result Eq. 4 is expressed as:

$$F_{chain}(L-l) \cong \frac{k_B T}{b}\Omega(L-l)(1-\xi^{-1}) \quad (12)$$

The constant $A$ in Eq. 11 then becomes:

$$A = \frac{l_p b}{R^2} - \ln(\kappa R) - \Omega(1-\xi^{-1}) \quad (13)$$

## Results and discussion

### Dendrimers regarded as non-penetrable spheres

The optimal wrapping length of DNA around a dendrimer ($l_{opt}$) can be estimated according to the analytical model by taking the first derivative of the free energy ($F$, Eq. 11), with respect to the wrapping length ($l$), and solving the equation $dF/dl$=0 for $l_{opt}$. This requires, however, that the number of dendrimers bound per DNA molecule is known. Here we use the experimental value, $N_{exp}$, ($r_{charge}$<1) and substitute $N$ for this value in the equation to estimate $l_{opt}$ containing a G2, G4, G6, or G8 dendrimer. Since $N_{exp}$ was not available for G1 dendrimers, the analytical model was not applied in this case. The dendrimer-dendrimer spacing $D(N,l)$ is set to $(L - Nl + 2NR)/N$ for hard (non-penetrable) spheres. This means that $R = R_o$ (Table 1) for the calculation of the dendrimer/DNA aggregate free energy as described above. Table 3 shows that the optimal DNA wrapping length increases for higher dendrimer generations. The difference ($Dif$) between $l_{opt}$ and the isoelectric length of DNA, $l_{iso}$, also increases as a function of dendrimer generation. The $l_{iso}$ values are shown in Table 1 for all dendrimer generations studied experimentally. Table 3 also shows that the effective charge of the dendrimer/DNA complexes, $Z^*$, is negative for all dendrimer generations and increases for larger dendrimers. The charge of the individual dendrimer in the complex is therefore reversed, giving a negative value of the ratio between the charge of the dendrimer/DNA complex and the charge of the dendrimer alone, $Z^*/Z$. It is interesting to note that the analytical model values for the dendrimer/DNA complexes composed of a G2, G4, or G6 dendrimer correspond to that of a nucleosome, which has a net negative charge $Z^*$ and $Z^*/Z$=-0.15.[28] The complex formed with a G8 dendrimer shows the most negative value, however, $Z^*/Z$ indicates that the complex is nearly neutralized. As will be discussed further below the negative net charge is in agreement with the negative zeta potential values obtained. The center-to-center dendrimer spacing in a dendrimer/DNA aggregate, $D(N,l)=(L-Nl+2NR)/N$, increases as the dendrimer generation increases. $D'$, which is the length of the DNA linking two neighboring dendrimers, was found to increase with the dendrimer generation, except for G4 where an unphysical negative value was found. This results from the fact that the total DNA wrapping length, i.e. the DNA around the 140 G4 dendrimers (the number of complexes that constitute the aggregate), is larger than the DNA contour length. The quantity $(D'+Dif)\cdot N/L$ describes the fraction of the DNA strand (with length, $L$) not needed to neutralize the dendrimer charge. It is calculated from the sum of the DNA linker lengths and the difference between the optimal wrapped DNA lengths and the lengths needed to neutralize the dendrimer charges. As an example, 59% of the DNA is neutralized in a G2/DNA aggregate (and the complex is net negative). G4/DNA aggregates are, however, slightly positive (=294 $e$). This should be compared to the Manning counterion condensation theory, which predicts that about 90% of the DNA charges need to be neutralized for the DNA to condense.[19]

The ratio between $l_{opt}$ and the dendrimer circumference ($2\pi R$), i.e. the number of turns that the DNA is able to wrap around the dendrimer, increases with the dendrimer size (Table 3). The less efficient charge neutralization found for G2 dendrimers can be ascribed to their larger curvature and the stiffness of the DNA. The inter-particle repulsive interaction, between complexes, is therefore more pronounced. As a result the smaller dendrimers are expected to decorate the DNA molecule instead of the DNA being wrapped around the dendrimer. The higher generation dendrimers, G6 and G8, which have lower curvature and higher surface charge density, are, however, able to interact more effectively with the oppositely charged DNA. The DNA therefore wraps the larger dendrimer to a higher extent, that is, more than one turn as obvious from the increased value of $l_{opt}/2\pi R$.

**Table 3.** Analytical model results for the interaction between dendrimers and DNA of contour length $L$= 1472.5 nm. Dendrimers are considered to be hard spheres of radius $R = R_o$[a].

| | Dendrimer | | | |
|---|---|---|---|---|
| | G2 | G4 | G6 | G8 |
| $l_{opt}$ ($nm$) | 3.2 | 12.2 | 50.4 | 182.8 |
| $Dif$ ($nm$) | 0.5 | 1.4 | 6.8 | 8.8 |
| $Z^*$ | -3 | -8 | -40 | -51 |
| $Z^*/Z$ | -0.19 | -0.13 | -0.16 | -0.05 |
| $D(N,l)$ ($nm$) | 4.3 | 2.8 | 48.4 | 121.4 |
| $D'=D-2R$ ($nm$) | 1.4 | -1.7 | 44.5 | 139.6 |
| $(D'+Dif)N_{exp}/L$ | 0.41 | -0.03 | 0.56 | 0.5 |
| $l_{opt}/2\pi R$ | 0.35 | 0.86 | 2.38 | 5.99 |
| $F_{int}/F_{min}$ | 0.004 | 0.009 | 0.019 | 0.004 |

[a] The number of dendrimers per DNA, $N$, is set equal to $N_{exp}$, Table 2. $l_{opt}$ is the DNA wrapping length per dendrimer. The difference between the optimal wrapped DNA length and the length needed to neutralize the dendrimer charges is $Dif = l_{opt}-l_{iso}$. $Z^*$ is the charge of the complex and $Z$ is the charge of the dendrimer, see Table 1. The center-to-center dendrimer spacing is given by $D(N,l)$, $D'$ is the length of the DNA linking two neighboring dendrimers, and $l_{opt}/2\pi R$ is, approximately, the number of DNA turns around each dendrimer. $(D'+Dif)N_{exp}/L$ describes the fraction of the DNA strand (with length, $L$) not needed to neutralize the dendrimer charge. $F_{int}$ is the electrostatic repulsion between complexes and $F_{min}$ is the minimal total free energy of the system.

### Dendrimers regarded as penetrable spheres

As a first step the simple model presented above assumes that the dendrimers are hard spheres. However, dendrimers are known to be soft and flexible.[49-51] Their internal structure and size are controlled not only by molecular architecture but also by the intramolecular electrostatic repulsions. One would

therefore expect that the dendrimers contract upon interaction with an oppositely charged DNA molecule. The simplest way to take this effect into account in Eq. 11 is to vary the radius ($R$=x$R_o$) of the dendrimers. A reduced dendrimer size will affect the distance between two dendrimers, the DNA wrapping length, and, concomitantly, the charge of the complex. The results from calculating the DNA wrapping length for dendrimers of varying radius and generation are shown in Tables 4–7.

**Table 4.** Analytical model results for the interaction between G2 dendrimers and DNA of contour length $L$= 1472.5 nm. The results of the interaction are modeled as a function of the dendrimer radius $R$ =x$R_o$[a], where $R_o$=1.45 nm

| | Fraction, $x$, of G2 dendrimer radius, $R_0$=1.45 nm Penetration to radius $R$=$xR_0$ | | | | | | |
|---|---|---|---|---|---|---|---|
| | 1 | 0.9 | 0.8 | 0.7 | 0.6 | 0.5 | 0.4 |
| $l_{opt}$ (*nm*) | 3.2 | 2.8 | 2.2 | 1.6 | 1.0 | 0.2 | -0.8 |
| *Dif* (*nm*) | 0.5 | ≈0.0 | -0.5 | -1.1 | -1.8 | -2.5 | -3.5 |
| *Z** | -3 | -0.2 | 3 | 6 | 10 | 15 | 20 |
| *Z*/Z* | -0.18 | -0.01 | 0.18 | 0.37 | 0.62 | 0.93 | 1.25 |
| *D*(*N*,*l*) (*nm*) | 4.3 | 4.5 | 4.7 | 5.0 | 5.4 | 5.9 | 6.5 |
| *D´=D-2R* (*nm*) | 1.4 | 1.88 | 2.41 | 3.02 | 3.68 | 4.44 | 5.38 |
| $N_{exp}$(*D´+Dif*)/*L* | 0.41 | 0.41 | 0.41 | 0.41 | 0.41 | 0.41 | 0.41 |
| $l_{opt}/2\pi R$ | 0.35 | 0.33 | 0.3 | 0.25 | 0.17 | 0.04 | -0.3 |
| $F_{in}/F_{min}$ | 0.004 | 0 | 0.005 | 0.03 | 0.117 | 0.327 | 0.7 |

[a] The parameters are defined in the footnote of Table 1 and 3.

**Table 5.** Analytical model results for the interaction between G4 dendrimers and DNA of contour length $L$= 1472.5 nm. The results of the interaction are modelled as a function of the dendrimer radius $R$ =x$R_o$[a], where $R_o$=2.25 nm.

| | Fraction, $x$, of G4 dendrimer radius, $R_0$=2.25 nm Penetration to radius $R$=$xR_0$ | | | | | | |
|---|---|---|---|---|---|---|---|
| | 1 | 0.9 | 0.8 | 0.7 | 0.6 | 0.5 | 0.4 |
| $l_{opt}$ (*nm*) | 12.2 | 12.0 | 11.6 | 11.3 | 11.0 | 10.4 | 9.4 |
| *Dif* (*nm*) | 1.4 | 1.1 | 0.8 | 0.5 | 0.1 | -0.4 | -1.5 |
| *Z** | -8 | -6 | -5 | -3 | -0.59 | 2 | 9 |
| *Z*/Z* | -0.12 | -0.09 | -0.07 | -0.04 | -0.01 | 0.03 | 0.14 |
| *D*(*N*,*l*) (*nm*) | 2.8 | 2.6 | 2.5 | 2.3 | 2.2 | 2.3 | 2.9 |
| *D´=D-2R* (*nm*) | -1.7 | -1.4 | -1.1 | -0.8 | -0.5 | 0.1 | 1.1 |
| $N_{exp}$(*D´+Dif*)/*L* | -0.035 | -0.035 | -0.035 | -0.035 | -0.034 | -0.034 | -0.034 |
| $l_{opt}/2\pi R$ | 0.86 | 0.93 | 1.03 | 1.14 | 1.29 | 1.47 | 1.66 |
| $F_{in}/F_{min}$ | 0.009 | 0.002 | 0 | 0.001 | 0 | 0.001 | 0.001 |

[a] The parameters are defined in the footnote of Table 1 and 3.

**Table 6.** Analytical model results for the interaction between G6 dendrimers and DNA of contour length $L$= 1472.5 nm. The results of the interaction are modeled as a function of the dendrimer radius $R$ =x$R_o$[a], where $R_o$=3.35.

| | Fraction, $x$, of G6 dendrimer radius, $R_0$=3.35 nm Penetration to radius $R$=$xR_0$ | | | | | | |
|---|---|---|---|---|---|---|---|
| | 1 | 0.9 | 0.8 | 0.7 | 0.6 | 0.5 | 0.4 |
| $l_{opt}$ (*nm*) | 50.4 | 49 | 47.4 | 46.4 | 45.4 | 44.7 | 43.6 |
| *Dif* (*nm*) | 6.8 | 5.5 | 3.9 | 2.9 | 1.8 | 1.1 | ≈0 |
| *Z** | -40 | -32 | -23 | -17 | -11 | -7 | -0.23 |
| *Z*/Z* | -0.15 | -0.12 | -0.08 | -0.06 | -0.04 | -0.02 | -0.001 |
| *D*(*N*,*l*) (*nm*) | 48.4 | 49.1 | 49.9 | 50.3 | 50.7 | 50.7 | 51.2 |
| *D´=D-2R* (*nm*) | 44.5 | 45.9 | 47.6 | 48.6 | 49.8 | 50.5 | 51.7 |
| $N_{exp}$(*D´+Dif*)/*L* | 0.56 | 0.56 | 0.56 | 0.56 | 0.56 | 0.56 | 0.56 |
| $l_{opt}/2\pi R$ | 2.38 | 2.58 | 2.81 | 3.14 | 3.58 | 4.23 | 5.16 |
| $F_{in}/F_{min}$ | 0.019 | 0.012 | 0.006 | 0.003 | 0.001 | 0.001 | 0 |

[a] The parameters are defined in the footnote of Table 1 and 3.

**Table 7.** Analytical model results for the interaction between G8 dendrimers and DNA of contour length $L$= 1472.5 nm. The results of the interaction are modelled as a function of the dendrimer radius $R$ =x$R_o$[a], where $R_o$=4.85.

| | Fraction, $x$, of G8 dendrimer radius, $R_0$=4.85 nm Penetration to radius $R$=$xR_0$ | | | | | | |
|---|---|---|---|---|---|---|---|
| | 1 | 0.9 | 0.8 | 0.7 | 0.6 | 0.5 | 0.4 |
| $l_{opt}$ (*nm*) | 182.8 | 182.2 | 180.0 | 179.0 | 177.8 | 176.0 | 175.0 |
| *Dif* (*nm*) | 8.8 | 8.1 | 5.9 | 4.9 | 3.7 | 1.9 | 0.9 |
| *Z** | -51 | -48 | -35 | -29 | -22 | -11 | -5 |
| *Z*/Z* | -0.04 | -0.04 | -0.03 | -0.02 | -0.02 | -0.01 | -0.005 |
| *D*(*N*,*l*) (*nm*) | 121.4 | 121.1 | 122.3 | 122.3 | 122.5 | 123.3 | 123.4 |
| *D´=D-2R* (*nm*) | 139.6 | 140.4 | 143.1 | 144.4 | 145.9 | 148.1 | 149.4 |
| $N_{exp}$(*D´+Dif*)/*L* | 0.5 | 0.5 | 0.51 | 0.51 | 0.51 | 0.51 | 0.51 |
| $l_{opt}/2\pi R$ | 5.99 | 6.63 | 7.37 | 8.38 | 9.7 | 11.53 | 14.3 |
| $F_{in}/F_{min}$ | 0.004 | 0.003 | 0.002 | 0.001 | 0.001 | 0 | 0 |

[a] The parameters are defined in the footnote of Table 1 and 3.

The optimal DNA wrapping length, $l_{opt,}$ is shown to decrease with the dendrimer radius. The dendrimer radius (penetration) effect on $l_{opt}$ is, furthermore, smaller for the lower generation dendrimers, i.e. G2 and G4, than for G6 and G8. It should be noted that the $l_{opt}$ value for the G2/DNA aggregates for x = 0.4 is negative (Table 4), which is obviously not physically possible. The difference (*Dif*) between $l_{opt}$ and $l_{iso}$ decreases for all dendrimer generations when the radius of the dendrimer decreases. For G2 and G4 *Dif* turns negative at x = 0.8 and 0.5, respectively. The larger dendrimers always gives $l_{opt} > l_{iso}$ for all used dendrimer radii values, i.e. the degree of penetration. As a result, the net charge of the complexes, *Z**, composed of G2 or G4 dendrimers turns from being negative to positive when the dendrimer radius decreases. For dendrimers of higher generations *Z** is negative for all values of x, that is, charge inversion is obtained for all considered dendrimer radii.This suggests that the degree of dendrimer penetration does not affect the charge reversal. The *Z*/Z* ratio decreases when the dendrimer generation increases and is, in general, small, i.e., the electrostatic repulsion between complexes is low.

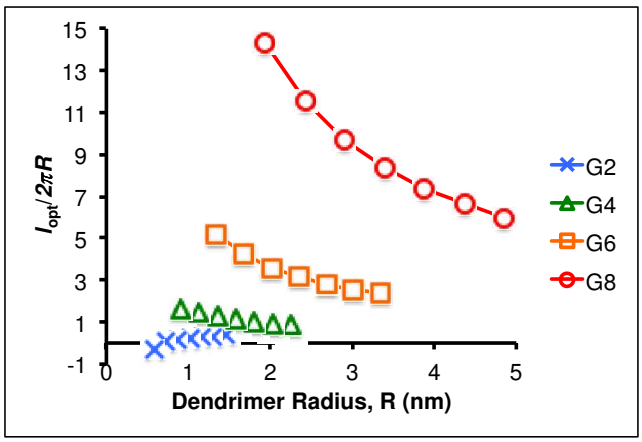


**Figure 2.** The ratio between the optimal DNA wrapping length and the circumference of the dendrimer, $l_{opt}/2\pi R$, as a function of dendrimer radius for different dendrimer generations, *G*.

As expected the $(D´+Dif)*N/L$ ratio is independent of the dendrimer radius as the value of $D´$ increases with the same amount as *Dif* decreases. Figure 2 shows the ratio between the optimal DNA wrapping length and the circumference of the dendrimer, $l_{opt}/2\pi R$, as a function of dendrimer radius for different generations, *G*. In general, the decrease in the radius of the dendrimers leads to a larger number of DNA turns around the dendrimers ($l_{opt}/2\pi R$), with the exception of G2 dendrimers. Here, it should be recalled that the charge of the dendrimer remains the same as the radius is decreased and the number of DNA turns wrapped around the dendrimer is always larger for the higher generation, even if the apparent radius is the same. Contrary to the higher generation dendrimers, the number of turns around the G2 dendrimers decreases slightly when the dendrimer contracts. The decrease in the DNA optimal wrapping length relative to the decrease of the G2 dendrimer size is furthermore large (Table 4). The opposite trend was observed for higher generation dendrimers, where the decrease of the optimal wrapping length compared to the dendrimer size is not as pronounced. These differences are expected to be related to the smaller size of the G2 dendrimer. The cost in free energy to bend the DNA strand to the required curvature, $F_{elastic}$, is concluded to be too high relative to the gain by neutralizing the DNA chain with the oppositely charged dendrimer. This is also the reason why a negative value for a 60% decrease of the G2 dendrimer radius was observed. It is worth to note from Tables 3-7 that the electrostatic interaction between complexes, $F_{int}$, for realistic values of *R*, is relatively small or negligible in comparison with the electrostatic interaction between the DNA and the dendrimer in the complex. Thus, it is assumed that this interaction is not likely to introduce any errors of significance in our calculations.

**Relation between the wrapping of DNA and the observed morphologies of DNA/dendrimer aggregates**

Our modelling data shows that DNA wraps less than one turn around the lower generation dendrimers. In fact G2 can be regarded as decorating the DNA chain (Figure 3). It is therefore not surprising that the predominant aggregate morphologies in samples containing DNA and low generation dendrimers, as visualized using cryo-TEM, were rods and toroids.[39] For toroidal aggregates to form, the electrostatic attraction is expected to have to be moderate such that a balance between mobility and high affinity binding of the DNA to the dendrimer exists. Toroidal morphologies have been reported in vivo, for example in some phages and vertebrate sperm cells. [47,48] They are often internally organised as hexagonal DNA arrays in order to allow for high density packing.

The higher generation dendrimers, G6 and G8, have both lower curvature and higher surface charge density. They are therefore able to interact more effectively with the DNA charges at the same time as the free energy cost of bending the DNA is less than for lower generation. Therefore DNA is able to wrap the larger dendrimer several turns, e.g. more than 5 turns for G8 as illustrated in Figure 3. Consequently, cryo-TEM images displaying more globular and disordered aggregates.[39] Manning also reported that the curvature and the charge of the macroion, ionic strength and the bending elasticity of the polyelectrolyte limit the stability of the complex.[19]

It is clear that highly ordered rods and toroids are found for low generation dendrimers, where the DNA wraps less than one turn around the dendrimer. However disordered globular structures appear for high generation dendrimers, where DNA wraps several turns around the dendrimer. From Table 5 we note that the net charge of the complex with G4 dendrimers is close to zero. Furthermore DNA wraps about one turn around each G4 dendrimer. These findings are interesting, as G4 has been shown experimentally to form a variety of different morphologies, that is, it behaves like a border case, allowing for higher flexibility in terms of structure and shape compared to other generations studied. [39]

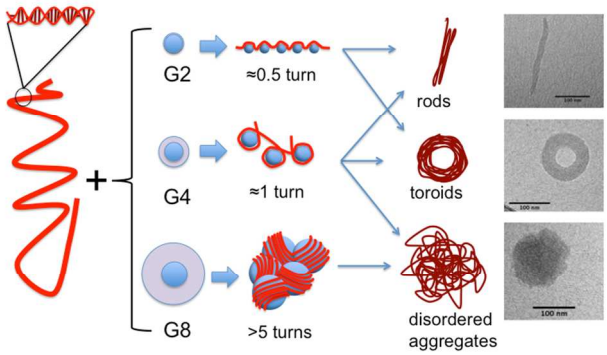


**Figure 3.** Schematic figure that depicts the relation between the wrapping of the DNA and morphology of the formed complexes. The number of turns the DNA can wrap the dendrimer, i.e. $l_{opt}/2\pi R$ as given in Tables 4-7, are also indicated. Note that G4 is the border case, where different morphologies can form. The cryo-TEM images are adopted from Ainalem et al.[39]

**Table 8.** The calculated charge of the complexes and the linkers between adjacent complexes $e(Z^{*}+ Z_{D^{-}})$ in a dendrimer/DNA aggregate composed of one DNA molecule with contour length 1472.5 nm and a multiple of dendrimers. Values for G2, G4, G6 and G8 dendrimers are presented for different dendrimer radii, $R=xR_0$. The values were estimated by using the calculated wrapping lengths shown in Tables 4-7.

| Dendrimer | Charge | Fraction, *x*, of dendrimer radius to which penetration occurs | | | | | | |
|---|---|---|---|---|---|---|---|---|
| | | 1 | 0.9 | 0.8 | 0.7 | 0.6 | 0.5 | 0.4 |
| G2 | $Z^*$ | -3 | ≈0 | 3 | 6 | 10 | 15 | 20 |
| | $Z_{D'}$ | -8 | -11 | -14 | -17 | -21 | -26 | -31 |
| | $Z^*+Z_{D'}$ | -11 | -11 | -11 | -11 | -11 | -11 | -11 |
| G4 | $Z^*$ | -8 | -6 | -5 | -3 | -1 | 2 | 9 |
| | $Z_{D'}$ | 10 | 8 | 7 | 5 | 3 | 0 | -7 |
| | $Z^*+Z_{D'}$ | 2 | 2 | 2 | 2 | 2 | 2 | 2 |
| G6 | $Z^*$ | -40 | -32 | -23 | -17 | -11 | -7 | ≈0 |
| | $Z_{D'}$ | -261 | -270 | -279 | -286 | -292 | -297 | -304 |
| | $Z^*+Z_{D'}$ | -301 | -302 | -202 | -203 | -203 | -304 | -304 |
| G8 | $Z^*$ | -51 | -48 | -35 | -29 | -22 | -11 | -5 |
| | $Z_{D'}$ | -821 | -825 | -841 | -849 | -858 | -871 | -878 |
| | $Z^*+Z_{D'}$ | -872 | -873 | -876 | -878 | -880 | -882 | -883 |

[a]Data for the expected charge of a dendrimer/DNA aggregate, calculated based on the number of dendrimers per DNA molecule.

**Table 9.** The calculated charge of a dendrimer/DNA aggregate is presented as a function of dendrimer generation. Experimental values are presented for comparison.

| | *G2*/DNA (*e*) | *G4*/DNA (*e*) | *G6*/DNA (*e*) | *G8*/DNA (*e*) |
|---|---|---|---|---|
| Calculated | -3498 | 280 | -4563 | -3539 |
| Experimental[a] | -3574 | 298 | -4566 | -3542 |

[a]Data reproduced from Ainalem et al.[36,37]

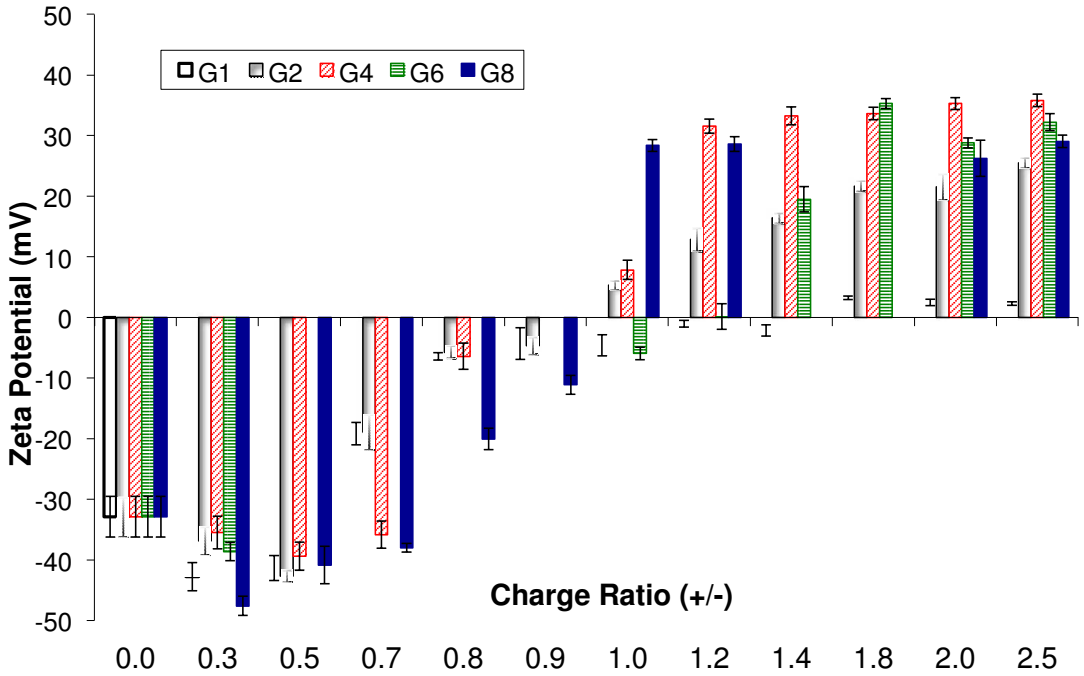


**Figure 4.** The zeta potential of aggregates formed between DNA of 4331 bp and PAMAM dendrimers of generation 1, 2, 4, 6 and 8 in the presence of 10 mM NaBr. Data is presented over a range of charge ratios ($r_{charge}$) and the pH of solutions was 7.00 ± 0.3.

**Charge of the dendrimer/DNA aggregates**

The model presented above captures some features on the interaction between DNA and dendrimers, and gives a realistic account for the complexes formed when a DNA segment wraps around one dendrimer. For gene delivery applications the charge of the complexes is an important parameter and can be estimated based on the DNA wrapping length. Table 8 shows the calculated charge of the complexes and the linkers between adjacent complexes $e(Z^*+Z_{D'})$ in a dendrimer/DNA aggregate composed of one DNA molecule with contour length 1472.5 nm and a multiple of dendrimers. Values for G2, G4, G6 and G8 dendrimers are presented for different dendrimer radii, $R=xR_0$. From Table 8 it can be concluded that the net charge of one complex and one linker does not change when the

dendrimer size is decreased. For x= 1 these charges are -11*e*, +2*e*, -301*e*, and -872*e* for G2, G4, G6, and G8 dendrimers respectively. From these values the net charge of the aggregates can furthermore be estimated by taking into account the number of dendrimers bound per one DNA, see Table 9 which also shows experimental data. The net charge is negative for all the dendrimer generations except for aggregates composed of G4 dendrimers, for which the net charge is slightly positive.

Another way to estimate the dendrimer/DNA aggregate charge is to measure its surface potential. For this purpose, zeta potential measurements were performed on DNA-containing aggregates in aqueous solutions of 10 mM NaBr. As a result of the cooperative nature of the dendrimer/DNA aggregation process for low $r_{charge}$ values, no free dendrimers exist in the presence of condensed DNA.[38,39] No contribution to the zeta potential from free dendrimers should therefore exist. However, at low $r_{charge}$, free DNA exists in equilibrium with the dendrimer/DNA aggregates. It is important to note that Dynamic light scattering (DLS) experiments have shown that free DNA has two relaxation modes; a slow translational diffusion mode and a fast mode arising from the internal motions of the DNA coil.[52-54] Upon DNA aggregation, i.e. increasing $r_{charge}$, DLS experiments showed that the internal motions of the DNA coil decreased and disappeared.[39] This is related to the formation of DNA-containing aggregates with negligible internal motions.[55] For $r_{charge}\approx1$ the amount of free DNA is therefore expected to be small. The translational diffusion for the aggregate and the free DNA are furthermore sufficiently well separated for the recorded zeta potential to mainly reflect the dendrimer/DNA aggregates.[39] Theoretically, the internal motions of DNA should not affect the zeta potential as it is a measure of surface charge.

Figure 4 shows the results of zeta potential measurements for dendrimer/DNA aggregates formed at varying $r_{charge}$ and for varying dendrimer generation. The zeta potential was found to be highly negative for $r_{charge}<1$, which is in good agreement with the calculated aggregate charges, with maximum negative values occurring at $r_{charge}$ values of 0.3 and 0.5. These results signify a negative surface charge of the aggregates and high colloidal stability, in good agreement with previous experimental data showing the existence of stable dispersions of rod-like and toroidal morphologies in the G1/DNA and G2/DNA systems.[39,44,45] Such structures are believed to contain regions of linker DNA due to the sparsity of the dendrimers and thus are expected to be predominantly negative. Around charge neutrality ($r_{charge}=1$), low zeta potential values relating to neutral surface charge were found for all generations. Aggregation in the samples was also noted at $r_{charge}=1$ confirming the low colloidal stability as indicated by the zeta potential values. The fact that aggregation occurred at theoretical charge neutrality infers that all the surface primary amine groups on the dendrimers are protonated at pH 7. For $r_{charge}>1$ the zeta potential turned positive and increased with increasing $r_{charge}$ until reaching a plateau. At this stage the aggregates display again good colloidal stability and the results indicate an overcharging of the systems. Note that the plateau is reached first for the G8/DNA system, while G1/DNA shows the smallest overcharging. This has been shown experimentally,[56] and resorting to Monte Carlo simulations of linear polyelectrolytes.[57] It is noteworthy that the plateau for the cationic aggregates is reached for $r_{charge}\approx1.2$ and 1.0 for for G4 and G8, respectively. For these two DNA-containing aggregates the magnitude of the zeta potential is about the same. The aggregates formed with G6 reaches the plateau at significantly higher charge ratio, $r_{charge}\approx1.8$. We have previously observed that there is a significant difference in the morphology of the dendrimer/DNA aggregates depending on the dendrimer generation.[39] G1/DNA aggregates remained, however, unstable at charge neutrality as well as for $r_{charge}>1$, which suggests that the four positive charges it bares are not enough to induce overcharging of DNA. G2 forms rod-like or toroidal structures, while G6 and G8 form more globular aggregates. G4 forms multiple complex structures; toroids, rods and globular structures for lower $r_{charge}$.[39] We note that the experimental data for the number of dendrimers bound to a DNA molecule would imply that the G4-containing aggregates would be more cationic than the other dendrimer-containing aggregates. This is not observed in the zeta potential measurement. Possibly this has to do with the fact that G4/DNA aggregates exhibit a range of different morphologies which might affect both binding and zeta potential data. We also note that the zeta potential for the G2/DNA aggregates is very dependent on the $r_{charge}$. One factor that might be linked to this observation is that G2 shows a decrease in the optimal wrapping length with the dendrimer radius (or penetration) compared to the opposite trend for aggregates formed with higher generation dendrimers. As discussed above the cost in free energy to bend the DNA strand to the required curvature for this small dendrimer can be expected to be too high. It is also interesting to note that this finding, that is the implication that the composition of G2/DNA aggregates and hence also their zeta potential can more readily adopt to the $r_{charge}$ compared to dendrimer/DNA aggregates containing other generations, shows good agreement with previous experimental data showing that the morphology of G2/DNA aggregates changes with time, contrary to higher generations that seem to be kinetically trapped.[44]

## Conclusions

For the theoretical model applied in this study, modified to take into account that dendrimers are penetrable and soft, we conclude that the number of DNA turns around a dendrimer increases with the dendrimer size or generation. This finding is in agreement with experimental studies by Ainalem et al. and Carnerup et al. reporting on dendrimer/DNA aggregate morphologies.[39,44,45] The relation between the wrapping of DNA and the observed morphologies in previous work can be rationalized in context of the extent of wrapping of the DNA around the dendrimer. The highly ordered rods and toroids found for low generation dendrimers, can be attributed to the fact that the DNA wraps less than one turn around the dendrimer. Consequently the disordered globular structures that appear for high generation dendrimers, is likely a consequence of the wrapping of DNA in several turns around these dendrimers. Particularly noteworthy is that the dendrimer generation 4 complexes, where the DNA wraps about one turn around the dendrimers, are the borderline case and can form all types of morphologies. We also note that for $r_{charge}<1$ the net charge of the dendrimer/DNA aggregates is negative for all generations except for generation 4 where the value is slightly positive.

The number of dendrimers per DNA molecule decreases for increasing dendrimer generations, and the net aggregate charge is independent of the state of the dendrimer, i.e., if it is contracted or not.

The theoretical study showed furthermore that the net charge of dendrimer/DNA complexes, which consist of one dendrimer

and the segment of the DNA molecule in contact with the dendrimer, is negative for the higher generation dendrimers and also independent of the dendrimer radius for a specific generation. The net charge of the dendrimer/DNA complexes composed of lower dendrimer generations, however, changes from negative to positive as the dendrimer is unable to retain its original radius and becomes contracted.

Figure 4 visualizes the dendrimer size within a dendrimer/DNA complex for $x$=1.0, the hard sphere model, and for the soft sphere model, where the reduction of the radius is the penetration required to arrive as close to charge neutrality of the complex as possible within the modelled range of penetration (Table 8, for $x$-values ranging from 0.4 to 1.0). For the highest dendrimer generations studied, G6 and G8, this means $x$=0.4. Figure 5 furthermore compares the $Z^*$ values obtained using the analytical model treating the dendrimer as a hard and a soft sphere, respectively, for optimal DNA wrapping lengths.

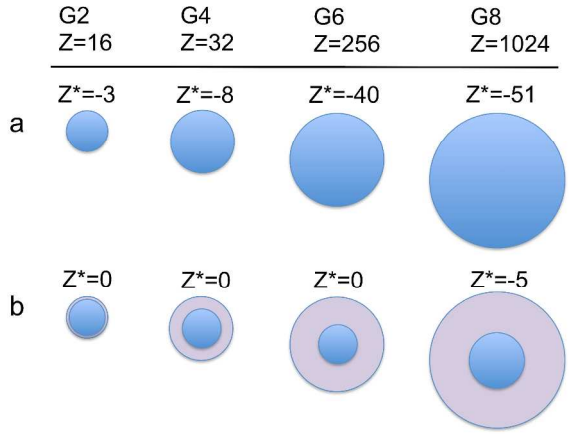


**Figure 5**. The effective charge of a dendrimer/DNA complex, Z*, and a visualization of the dendrimer size within the complex for optimal DNA wrapping lengths. In a) the dendrimer is treated as a hard, non-penetrable sphere and in b) the dendrimer is treated as a soft, penetrable sphere as close to charge neutrality of the complex as possible within the modeled range of penetration (Table 8). Z is the charge of the dendrimer alone.

In addition to the theoretical model, zeta potential measurements were performed on dendrimer/DNA aggregates composed of DNA (4331 bp) and positively charged PAMAM dendrimers of generation 1, 2, 4, 6 and 8. The surface charge measurements showed that the dendrimer/DNA aggregates have a net negative charge for all dendrimer generations when $r_{charge}$<1. The experimental data showed further that the aggregates display highly positive zeta potentials for higher $r_{charge}$ (>1), associated with positive surface charge and colloidal stability. Generation 1 remained, however, unstable past charge neutrality, which suggests that the four positive charges it bares are not enough to induce overcharging of DNA.

In this study we have focused on DNA interacting with oppositely charged dendrimers, but our approach could easily be extended and applied to any interacting system consisting of charged biopolymers and oppositely charged particles.

## Acknowledgements

The sixth EU framework program is acknowledged for work as being a part of a EU-STREP project with NEST program (NEONUCLEI, Contract 12967). The Linnaeus center of excellence on Organizing Molecular Matter through the Swedish Research Council as well as the Swedish Research Council are also thanked for financial support.

## Notes and references

[a] Physical Chemistry, Department of Chemistry, Lund University, P. O. Box 124, SE-221 Lund, Sweden. Fax: +46 46 2224413; Tel: +46 462228158; E-mail: Tommy.Nylander@fkem1.lu.se

[b] Physics Department, College of Science and Technology, Al_Quds University, Jerusalem, Palestine. E-mail: khawlaq@gmail.com

[c] School of Chemistry, University of Southampton, Highfield, Southampton, SO17 1BJ, United Kingdom. Fax: +44 23 8059 3781; Tel: +44 23 8059 3019; E-mail: gza@soton.ac.uk

[d] Biophysics and Medical Technology, Department of Physics, Norwegian University of Science and Technology, 7491 Trondheim, Norway. E-mail: rita.dias@ntnu.no

[e] European Spallation Source ESS AB, P.O Box 176, SE-221 00 Lund, Sweden. Tel: +46 46 888 30 74; E-mail: marie-louise.ainalem@esss.se

[*] Corresponding author.

1 1 M. Kralj and K. Pavelic, *EMBO Rep.* 2003, **4**, 1008-1012.
2 R. Duncan, *Pharm. J.* 2004, **273**, 485-488.
3 P. Kesharwani, K. Jain and N. K. Jain, *Prog. Polym. Sci.* 2014, **39**, 268– 307.
4 S. M. Moghimi, A. C. Hunter and J. C. Murray, *FASEB J.* 2005, **19**, 311-330.
5 S. Svenson and D. A. Tomalia, *Adv. Drug Delivery Rev.* 2005, **57**, 2106-2129.
6 J. F. Kukowska-Latallo, A. U. Bielinska, J. Johnson, R. Spindler, D. A. Tomalia and J.R. Baker, *Proc. Natl. Acad. Sci. U.S.A.* 1996, **93**, 4897-4902.
7 R. Esfand and D. A. Tomalia, *Drug Discovery Today* 2001, **6**, 427-436.
8 M. J. Cloninger, *Curr. Opin. Chem. Biol.* 2002, **6**, 742-748.
9 C. Dufes, I. F. Uchegbu, A. G. Schatzlein,. *Adv. Drug Delivery Rev.* 2005, **57**, 2177-2202.
10 P. Daftarian, A. E. Kaifer, W. Li, B. B. Blomberg, D. Frasca, F. Roth, R. Chowdhury, E. A. Berg, J. B. Fishman, H. A. A. Sayegh, P. Blackwelder, L. Inverardi, V. L. Perez, V. Lemmon, and P. Serafini. *Cancer Res.* 2011, **71**, 7452-7462.
11 H. C. Gérard, M. K. Mishra, G. Mao, S. Wang, M. Hali, J. A. Whittum-Hudson, R. M. Kannan, and A. P. Hudson, *Nanomed. Nanotechnol.* 2013, **9**, 996-1008
12 J. F. Kukowska-Latallo, A. U. Bielinska, J. Johnson, R. Spindler, D. A. Tomalia, and J. R. Jr. Baker, *Proc. Natl. Acad. Sci. U.S.A.* 1996, **93**, 4897-4902.
13 A. U. Bielinska, J. F. Kukowska-Latallo and J. R. Baker, *Biochim. Biophys. Acta* 1997, **1353**, 180-190.
14 P. Daftarian, A. Kaifer, W Li, B. Blomberg, D. Frasca, F. Roth, R Chowdhury, E. Berg, J. Fishman, H. Al Sayegh, P. Blackwelder, L. Inverardi, V. Perez, V. Lemmon, P. Serafini, *Cancer Research* 2011, **71**, 7452-7462.
15 M. A. Liu, *Immunity* 2010, **33**, 504–15.
16 R. K. Tekade, P. V. Kumar, N. K. Jain, *Chem Rev* 2009, **109**, 49–87.
17 G. Leroux-Roels, Vaccine 2010, **28**, 25–36.

18 R. W. Wilson and V. A. Bloomfield, *Biochemistry* 1979, **18**, 2192-2196.
19 G. S. Manning, *Q. Rev. Biophys.* 1978, **11**, 179-246.
20 K. Qamhieh and V. Lobaskin, *J. Phys. Chem. B* 2003, **107**, 8022-8029.
21 A. Akinchina and P. Linse, *Macromolecules* 2002, **35**, 5183-5193.
22 P. Chodanowski and S. *J.* Stoll, *Chem. Phys* . 2001, **115**, 4951-4960.
23 P. Chodanowski and S. Stoll, *Macromolecules* 2001, **34**, 2320-2328.
24 M. Johnsson and P. Linse, *J. Chem. Phys.* 2001, **115**, 10975-10985.
25 P. K. Maiti and B. Bagchi, *Nano Lett.* 2006, **6**, 2478-2485.
26 A. Akinchina and P. Linse, *J. Phys. Chem*. B 2003, **107**, 8011-8021.
27 T. T. Nguyen, A. Y. Grosberg and B. I. J. Shklovskii, Chem. Phys. 2000, **113**, 1110-1125.
28 T. T. Nguyen and B. I. Shklovskii, *Physica A* 2001, **293**, 324-338.
29 A. Y. Grosberg, T. T. Nguyen and B. I. Shklovskii, *Rev. Mod. Phys.* 2002, **74**, 329-345.
30 S. V. Lyulin and A. A. Darinskii, *Phys. Rev. E* 2008, **78**, 041801-1-041810-9.
31 K. Qamhieh, T. Nylander and M.–L. Ainalem, *Biomacromolecules* 2009, **10**, 1720-1726.
32 M. H. Chai, Y. H. Niu, W. J. Youngs and P. L. Rinaldi, *J. Am. Chem. Soc*. 2001, **123**, 4670-4678.
33 I. Lee, B. D. Athey, A. W. Wetzel, W. Meixner and J. R. Baker, *Macromolecules* 2002, **35**, 4510-4520.
34 A. M. Naylor, W. A. Goddard, G. E. Kiefer and D. A. Tomalia, *J. Am. Chem. Soc*. 1989, **111**, 2339-2341.
35 P. M. R. Paulo, J. N. C. Lopes and S. M. B. Costa, *J. Phys. Chem. B* 2007, **111**, 10651-10664.
36 S. Svenson and D. A. Tomalia, *Adv. Drug Del. Rev***.** 2005, **57**, 2106-2129.
37 D. A. Tomalia, *Prog. Poly Sci*., 2005, **30**, 294-324.
38 M.–L. Orberg, K. Schillen and T. Nylander, *Biomacromolecules* 2007, **8**, 1557-1563.
39 M.–L Ainalem, A. M. Carnerup, J. Janiak, V. Alfredsson, T. Nylander and K. Schillen, *Soft Matter*, 2009, **5**, 2310-2320.
40 K. Fant, E. K. Esbjörner, P. Lincoln and B. Nordén, *Biochemistry* 2008, **47**, 1732-1740.
41 M.-L. Ainalem, R. S. Dias, J. Muck, A. Bartles, D. Zink and T. Nylander, *PLOS ONE,* 2014, In press.
42 A. U. Bielinska, J. F. Kukowska-Latallo and J. R. Baker, *Biochem. Biophys. Acta* 1997, **1353**, 180-190.
43 H. Schiessel, R. F. Bruinsma and W. M. Gelbart, *J. Chem. Phys.* 2001, **115**, 7245- 7252.
44 A.M. Carnerup, M.-L. Ainalem, V. Alfredsson and T. Nylander, *Langmuir* 2009, **25**, 12466–12470.
45 A. M. Carnerup, M.-L. Ainalem, V. Alfredsson and T. Nylander, *Soft Matter* 2011, **7**, 760-768.
46 S. Alexander, P. M. Chaikin, P. Grant, G. J. Morales, P. Pincus and D. Hone, *J. Chem. Phys*. 1984, **80**, 5776-5781.
47 N. V. Hud, M. J. Allen, K. H. Downing, J. Lee and R. Balhorn, *Biochem. Biophys. Res. Commun.* 1993, **193**, 1347–1354.
48 N. V. Hud, *Biophys. J*. 1995, **69**, 1355–1362.
49 D. Potschke, M. Ballauff, P. Lindner, M. Fischer and F. Vogtle, *Macromol. Chem. Phys*. 2000, **201**, 330-339.
50 S. Rosenfeldt, N. Dingenouts, M. Ballauff, P. Linder, C. N. Likos, N. Werner and F. Vogtle, *Macromol. Chem. Phys*. 2002, **203**, 1995-2004.
51 C. N. Likos, S. Rosenfeldt, N. Dingenouts, M. Ballauff, N. Werner and F. Vogtle, *J. Chem. Phys*. 2002, **117**, 1869-1877.
52 S.A. Allison, S.S. Sorlie and R. Pecora, *Macromolecules* 1990, **23**, 1110-1118.
53 S.S. Sorlie and R. Pecora, *Macromolecules* 1988, **21**, 1437-1449.
54 S.S. Sorlie and R. Pecora, *Macromolecules* 1990, **23**, 487-497.
55 M. Cárdenas, K. Schillén, T. Nylander, J. Jansson and B. Lindman, *Phys. Chem. Chem. Phys.* 2004, **6**, 1603-1607.
56 V. A. Kabanov, V. G. Sergeyev, O. A. Pyshkina, A. A. Zinchenko, A. B. Zezin, J. G. H. Joosten, J. Brakman and K. Yoshikawa, *Macromolecules* 2000, **33**, 9587-9593.
57 R. S. Dias, P. Linse and A. A. C. C. Pais, *J. Comp. Chem.* 2011, **32**, 2697–2707.